22nd Australasian Fluid Mechanics Conference AFMC2020
Brisbane, Australia, 7-10 December 2020
https://doi.org/10.14264/b2c1622

Studying the natural convection problem in a square cavity by a new vorticity-stream-function approach

P. Mayeli[1], T. K. Tsai[1] and G. J. Sheard[1]

[1] Department of Mechanical and Aerospace Engineering, Monash University, VIC 3800, Australia

Abstract

In this study, a benchmark natural convection problem is studied under a Gay—Lussac type approximation incorporating centrifugal effects in the context of a new vorticity-stream-function approach. This approximation differs from the classic Boussinesq approximation in that density variations are considered in the advection term as well as the gravity term in the momentum equations. Such a treatment invokes Froude number as a non-Boussinesq parameter deviating results from the classic Boussinesq approximation. Numerical simulations of the natural convection in square cavity are performed up to $Ra = 10^6$ and $\varepsilon = 0.3$ at $Pr = 0.71$ via proposed formulation and results are compared against the conventional Boussinesq approximation in terms of the average and local Nusselt number and entropy generation. Comparing results indicate that, up to $Ra = 10^5$, mentioned approaches are showing almost identical performance, but as the Rayleigh number exceeds 10^5, formed thermal boundary layer under Gay—Lussac type approximation is slightly thicker compared to the Boussinesq approximation accompanied by a stronger velocity gradient.

Keywords

Gay—Lussac approximation; Boussinesq approximation; vorticity-stream-function approach.

Introduction

Traditionally, the Boussinesq approximation [1] is adopted for the numerical simulation of the natural convection problems. Ignoring density variations except in buoyancy term and treating the flow field as incompressible makes the classic Boussinesq approximation popular among researchers [2-4]. Simple implementation and great accuracy of performance for problems associated with small temperature difference are main advantages of the Boussinesq approximation.

The main assumption of the Boussinesq approximation (density variation confined to the buoyancy term) is established based on small density variations. In other words, applying the Boussinesq approximation to cases with large density variations produces inaccurate results [5]. Foundry processes and astrophysical MHD simulations are two samples of the natural convection phenomena that are accompanied by a large temperature differences [6]. In these situations, it is better to avoid the Boussinesq approximation and use other numerical approaches beyond the Boussinesq approximation for numerical simulation of the natural convection phenomena.

Available remedies to avoid the limitations of the Boussinesq approximation for numerical simulation of natural convection problems may be divided into two major categories: compressible and incompressible. One remedy in the incompressible category is the Gay—Lussac approach, which is developed based on considering density variations in any term in which density appears, i.e. continuity and the advection/convection terms of the momentum/energy equations, respectively. Such a treatment introduces the Gay—Lussac parameter as a product of thermal coefficient expansion and temperature difference ($Ga = \beta\Delta\theta$). In this state, a pre-factor of $(1 - Ga\Theta)$ acts as a modifier on the aforementioned terms in the governing equations. It can be shown that the Boussinesq approximation is recovered as $Ga \to 0$ [7].

Recently, a Gay—Lussac type approach in the context of primitive variables was proposed by Lopez *et al.* [8] for the treatment of rapidly rotating flows, in which instead of considering density variations in all terms of the governing equations containing density, buoyancy effects were extended just to the centrifugal part of the advection term to capture centrifugal effects in those rapidly rotating flows. This idea is continued in this study and a new formulation of the governing equations in the context of the secondary vorticity stream-function variables are presented. The new formulation is applied on the square cavity benchmark problem and obtained results are compared against the conventional Boussinesq approximation in terms of the average and local Nusselt number and entropy generation.

Governing equations

According to Lopez *et al.* [8], more accurate results may be obtained by extending density variations to the centrifugal part of the advection term for rapidly rotating flows. Let us start with steady-state form of the momentum equation

$$\frac{\rho}{\rho_0}(\boldsymbol{u}\cdot\nabla)\boldsymbol{u} = -\frac{1}{\rho_0}\nabla p + \nu\nabla^2\boldsymbol{u} + \frac{\rho}{\rho_0} g\, \boldsymbol{e}_g. \quad (1)$$

Substituting the density state relation $\rho/\rho_0 = 1 - \beta\theta$ and the modified pressure (p^*) defined as $p^* = p + \rho_0\phi$, where ϕ is the gravitational potential whose gradient opposes the gravitational acceleration vector into equation (1) yields

$$(\boldsymbol{u}\cdot\nabla)\boldsymbol{u} = -\frac{1}{\rho_0}\nabla p^* + \nu\nabla^2\boldsymbol{u} - \beta\theta g\boldsymbol{e}_g + \beta\theta(\boldsymbol{u}\cdot\nabla)\boldsymbol{u}. \quad (2)$$

Using dimensionless quantities

$$\boldsymbol{X} = \frac{\boldsymbol{x}}{L}, \boldsymbol{U} = \frac{\boldsymbol{u}L}{\alpha}, P = \frac{p^*L^2}{\rho\alpha^2}, \Theta = \frac{\theta}{\Delta\theta} = \frac{T-T_0}{T_h-T_c}, \quad (3)$$

one can derive the dimensionless form of the momentum equation for natural convection problems,

$$(\boldsymbol{U}\cdot\nabla)\boldsymbol{U} = -\nabla P + Pr\,\nabla^2\boldsymbol{U} - RaPr\Theta\boldsymbol{e}_g + Ga\Theta(\boldsymbol{U}\cdot\nabla)\boldsymbol{U}. \quad (4)$$

Equation (4) introduces the Prandtl number $Pr = \nu/\alpha$ characterising the ratio of the molecular to thermal dissipation, and the Rayleigh number $Ra = g\beta\Delta\theta {L_{\text{ref}}}^3/\nu\alpha$ characterising the ratio of buoyancy to viscous and thermal dissipation. The Gay—Lussac parameter may be expressed as $Ga = \beta\Delta\theta = FrRaPr$ in which Fr is the Froude number characterising ratio of inertia to gravitational effects ($Fr = \alpha^2/gL^3$). The Gay—Lussac parameter also may be expressed based on the relative temperature difference (ε) as $Ga = \beta\Delta\theta = (T_h - T_c)/T_o = 2\varepsilon$. Comparing two expressions of the Gay—Lussac parameter gives the following relation for the Froude number which matches its magnitude based on the given ε at each Ra and Pr

$$Fr = 2\varepsilon/RaPr. \quad (5)$$

Using the introduced expression of the Gay—Lussac parameter ($Ga = FrRaPr$), the momentum equation may be expressed as

$$(\boldsymbol{U}\cdot\nabla)\boldsymbol{U} = -\nabla P + Pr\,\nabla^2\boldsymbol{U} - RaPr\Theta\big(\boldsymbol{e_g} - Fr(\boldsymbol{U}\cdot\nabla)\boldsymbol{U}\big). \quad (6)$$

As can be seen, equation. (6) is consistent with the momentum equation under the Boussinesq approximation, except for the additional inertial buoyancy term on the right hand side. When expressed in this form, it is apparent that the action of this additional term is to modify the effective direction (and strength) of the gravity locally throughout the flow which is ignored in the conventional Boussinesq approximation. Indeed, regions which are experiencing higher spatial accelerations (described by $(\boldsymbol{U}\cdot\nabla)\boldsymbol{U}$) will experience deviations from the Boussinesq buoyancy approximation. The strength of these deviations relative to gravity is described by Fr, with $Fr \to 0$ (and $Ga \to 0$) recovering the classical Boussinesq approximation. Thus under this Gay—Lussac type approximation, governing equations in steady state form are expressed as [9-10]

$$\begin{cases} \nabla\cdot\boldsymbol{U} = 0, \\ (\boldsymbol{U}\cdot\nabla)\boldsymbol{U} = -\nabla P + Pr\,\nabla^2\boldsymbol{U} - RaPr\Theta\big(\boldsymbol{e_g} - Fr(\boldsymbol{U}\cdot\nabla)\boldsymbol{U}\big), \\ (\boldsymbol{U}\cdot\nabla)\Theta = \nabla^2\Theta. \end{cases} \quad (7)$$

Using the secondary variables, i.e. vorticity ($\omega = \partial V/\partial X - \partial U/\partial Y$) and stream-function ($U = \partial\psi/\partial Y\,; V = -\partial\psi/\partial X$), the scalar formulation of the governing equations under the Gay—Lussac approximation are expressed as (subscripts denote differentiation)

$$\begin{cases} \nabla^2\psi = -\omega \\ (1 - RaPrFr\Theta)\big(\psi_y\omega_x - \psi_x\omega_y\big) = Pr\,\nabla^2\omega + RaPr\Theta_x, \\ \psi_y\Theta_x - \psi_x\Theta_y = \nabla^2\Theta\cdot \end{cases} \quad (8)$$

Problem description and parameters definition

Natural convection in a square cavity driven by hot and cold side-walls is a popular benchmark problem. Here it is studied under the two mentioned approximations. A schematic of the square cavity configuration is shown in figure 1, presenting the thermal boundary conditions comprising two horizontal adiabatic boundaries, and hot and cold left and right boundaries, respectively. The applied boundary conditions for vorticity and stream-function are also shown in this figure.

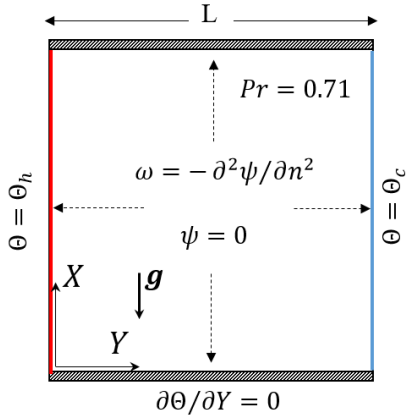

Figure 1. A schematic view of the problem and applied boundary conditions.

The local and average Nusselt number along the two constant-temperature walls are calculated as

$$Nu_{\mathrm{loc}}(Y) = -\frac{\partial\Theta}{\partial n}\Big|_{\mathrm{wall}}, \quad (9)$$

$$Nu_{\mathrm{avg}} = \int_0^1 Nu_{\mathrm{loc}}\,\mathrm{d}Y. \quad (10)$$

The dimensionless local entropy generation due to heat transfer (S_θ) and fluid friction (S_ψ) are calculated as

$$S_\Theta = \left[\left(\frac{\partial\theta}{\partial X}\right)^2 + \left(\frac{\partial\theta}{\partial Y}\right)^2\right], \quad (11)$$

$$S_\psi = \chi\left[2\left\{\left(\frac{\partial U}{\partial X}\right)^2 + \left(\frac{\partial V}{\partial Y}\right)^2\right\} + \left(\frac{\partial U}{\partial Y} + \frac{\partial V}{\partial X}\right)^2\right]. \quad (12)$$

In equation (11) χ is the irreversibility distribution ratio, which is assumed to be fixed and equal to 10^{-4} in this study. The total entropy generation due to heat transfer and fluid friction is calculated by the summation of the local entropy generation over the physical domain via

$$S_{\Theta,tot} = \int_V S_\Theta\,\mathrm{d}v, \quad (13)$$

$$S_{\psi,tot} = \int_V S_\psi\,\mathrm{d}v. \quad (14)$$

The relative dominance of entropy generation due to heat transfer and fluid friction is given by average Bejan number (Be_{avg}), a dimensionless parameter defined as

$$Be_{avg} = \frac{S_{\Theta,tot}}{S_{\Theta,tot}+S_{\psi,tot}}, \quad (15)$$

where $Be_{\mathrm{avg}} > 0.5$ implies dominance of heat transfer irreversibility and $Be_{\mathrm{avg}} < 0.5$ implies dominance of fluid friction irreversibility.

Results and discussion

Results obtained with the two approaches are presented in this section. Simulations are performed up to $Ra = 10^6$ and $\varepsilon = 0.3$ at a fixed Prandtl number $Pr = 0.71$. Based on equation (5) and according to the considered range of ε, the corresponding Froude number range is $0 \le Fr \le 0.6/RaPr$. The governing equations are solved using a control-volume finite element solver [11-18] with a second-order temporal accuracy. A mesh resolution study is performed and it is found that a mesh size of $n_x \times n_y = 121^2$ makes the problem independent of mesh size for both approximations in considered range of the Ra and ε.

For a better understanding of the added term effects in the momentum equation under the Gay—Lussac type approximation, the absolute magnitude of $\Theta\big(\psi_y\omega_x - \psi_x\omega_y\big)$ is portrayed in figure 2 for a Boussinesq case at $Ra = 10^6$. As seen, the magnitude of the non-Boussinesq acceleration is stronger at four corners of the cavity and weaker effects are sensible at central region of the physical domain. The stronger regions of non-Boussinesq effects are formed due to rapid fluid rotation near the four corners of the enclosure.

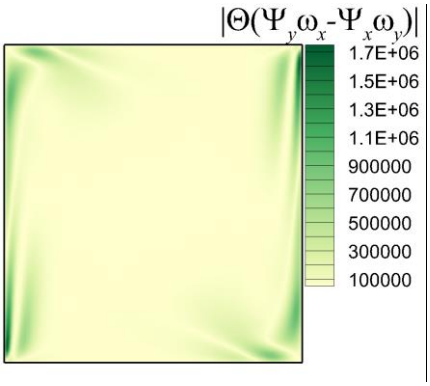

Figure 2. Magnitude of the acceleration vector field of the non-Boussinesq acceleration term i.e. $|\Theta\big(\psi_y\omega_x - \psi_x\omega_y\big)|$ at $Ra = 10^6$.

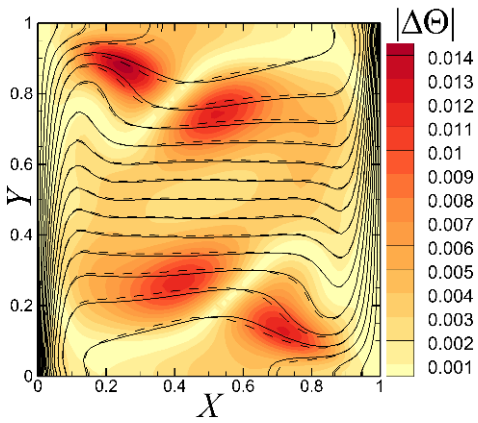

Figure 3. Absolute difference between temperature fields obtained from the Boussinesq and Gay—Lussac type approximations at $Ra = 10^6$. Solid lines are Boussinesq ($Fr = 0$) isotherms and dashed lines are isotherms of the Gay—Lussac type approximation at $Fr = 0.6/RaPr$.

The effects of the non-Boussinesq acceleration is sensed in figure 3 by depicting the absolute difference of temperature fields at $Ra = 10^6$ under the Boussinesq approximation ($Fr = 0$) and the Gay—Lussac type approximation with $Fr = 0.6/RaPr$. The maximum difference in this plot is approximately 0.015 that regarding the maximum value of Θ ($\Theta_{max} = 0.5$), it is showing a 3% mismatch between the two approaches ($|\Delta\Theta|_{max}/\Theta_{max} \cong 3\%$). It is clear that the mismatch between the two approaches increases with increasing non-Boussinesq parameter (Froude number).

Local Nusselt Number

Local Nusselt number distribution along the two vertical walls are presented at $Ra = 10^6$ for $Fr = 0, 0.3/RaPr$ and $0.6/RaPr$ under the two approximations in figure 4. For the left heating wall, by increasing the height and forming thicker thermal boundary, the total value of local Nusselt number is decreasing while this pattern is reverse for the right cooling part as the flow motion due to a clockwise rotation is downward along this wall. As seen, the difference of the local Nusselt number along the isotherm walls under two approximations is negligible in this problem, which is in agreement with presented absolute temperature difference field in Fig. 3 in which most of difference is occurring in the regions away from isotherm walls.

Average Nusselt Number

Computed average Nusselt number across $10 \leq Ra \leq 10^6$ is presented at $Fr = 0$ and $0.6/RaPr$ in figure 5 under the two approximations. Because of the similarity between the trends, results of $Fr = 0.3/RaPr$ are not shown in this plot. As expected, the average Nusselt number is increased by increasing the Rayleigh number. As expected, average Nusselt number values under two approximations are so close together as the local Nusselt number distributions were not showing significant difference. A quantitative investigation shows a small difference of 0.006% at the highest Rayleigh number between $Fr = 0$ and $Fr = 0.6/RaPr$ with a lower value for the Gay—Lussac type approximation compared to the Boussinesq approximation.

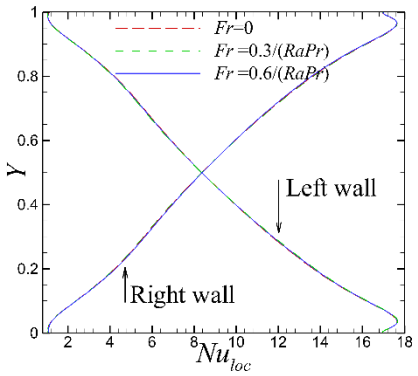

Figure 4. Local Nusselt number distribution along the vertical walls for different Froude numbers as stated at (a) $Ra = 10^6$ (b) $Ra = 10^5$.

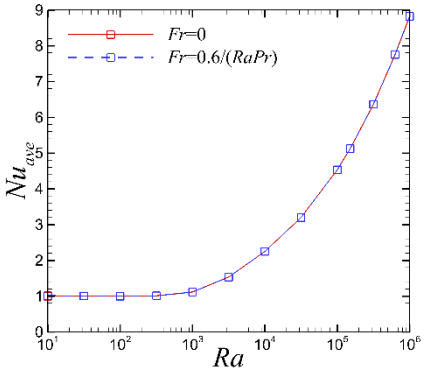

Figure 5. Average Nusselt number for $Fr = 0$ and $0.6/RaPr$ across $10 \leq Ra \leq 10^6$.

Average Bejan Number

The rate of entropy generation are shown in the context of average Bejan number under the two approximations at $Fr = 0$ and $0.6/RaPr$ in figure 6. Results indicate that up to $Ra \approx 10^3$, conduction is dominant part of heat transfer mechanism ($Be_{\text{avg}} \cong 1$). The average Bejan number intersects with $Be_{\text{avg}} = 0.5$ at $Ra \cong 2 \times 10^4$. This is where the share of both conduction and convection becomes equal in heat transfer mechanism, and thereafter the heat transfer mechanism becomes convection dominated with increasing Rayleigh number ($Be_{\text{avg}} < 0.5$). The difference of Be_{avg} between the two approaches becomes slightly different in the convection dominated regime for $Ra \geq 10^5$ with a lower value for the Gay—Lussac type approximation indicating slightly stronger velocity gradients under this approximation. The maximum difference between the two approaches at $Ra = 10^6$ is 0.2%.

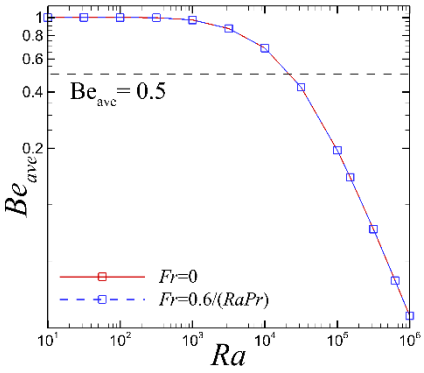

Figure 6. Average Bejan number for $Fr = 0$ and $0.6/RaPr$ across $10 \leq Ra \leq 10^6$.

Conclusion

In this paper, a new secondary variable formula is applied to the square cavity benchmark problem up to $Ra = 10^6$ and $\varepsilon = 0.3$ at $Pr = 0.71$. The new formula is a vorticity-stream-function expression of a Gay—Lussac type approximation which is derived by considering density variations in the advection term of the momentum equations in addition to the gravity term, offering an improved description of convection in rapidly rotating regions of the flow. A Froude number is introduced characterising deviation from the classic Boussinesq approximation as $Fr = 2\varepsilon/RaPr$. Obtained numerical data indicates that the Boussinesq approximation gives results consistent with the improved approximation up to $Ra = 10^5$ but as Rayleigh number exceeds 10^5, a slight mismatch between the two approaches is noticeable. At $Ra = 10^6$, a 0.006 % and 0.2 % difference is observed for the average Nusselt number and average Bejan number, under the classic Boussinesq approximation ($Fr = 0$) and the Gay—Lussac type approximation with $Fr = 0.6/RaPr$, respectively. In the context of the Gay-Lussac parameter, the present results demonstrate that the traditional Boussinesq approximation is accurate up to at least $\beta\Delta\theta = Ra\ Pr\ Fr = O(10^{-2})$, with deviations emerging beyond this magnitude. Finally, it is expected that non-Boussinesq effects will be significant at higher Rayleigh numbers, small-scale systems, or for fluids having large thermal expansion coefficients.

Acknowledgments

This research was supported by the Australian Research Council through Discovery Project DP180102647. P. M. is supported by a Monash Graduate Scholarship and a Monash International Postgraduate Research Scholarship. The authors are also supported by NCMAS grants providing access to the National Computational Infrastructure (NCI) and Pawsey Supercomputing Centre, supported by the Australian Government.

References

[1] Boussinesq, J. (1903) *Theorie Analytique de la Chaleur, vol. II*, Gauthier-Villars.

[2] Davis, G. (1983). Natural convection of air in a square cavity, a benchmark numerical solution. *Int. J. Numer. Methods Fluids*, 3, 249-264. (DOI: 10.1002/fld.1650030305).

[3] Wan, D.C., Patnail, B. S. V., Wei, G. W. (2001). A new benchmark quality solution for the buoyancy-driven cavity by discrete singular convolution. *Numer. Heat Transf. B* 40, 199-228. (DOI: 10.1080/104077901752379620).

[4] Ashrafizadeh, A., Nikfar, M. (2016). On the numerical solution of generalized convection heat transfer problems via the method of proper closure equations–part II: Application to test problems. *Numer. Heat Transf. B*, 70 (2) 204-222. (DOI: 10.1080/10407782.2016.1173467).

[5] Paillere, H., Viozat, C., Kumbaro, A., Toumi, I. (2000). Comparison of low Mach number models for natural convection problems, *Heat and mass transfer*, 36, 567-573 (DOI: 10.1007/s002310000116).

[6] Szewc, K., Pozorski, J., Tanière, A. (2011). Modelling of natural convection with Smoothed Particle Hydrodynamics: Non-Boussinesq formulation. *Int. J. Heat Mass Transf*, (54) 4807-4816. (DOI: 10.1016/j.ijheatmasstransfer.2011.06.034).

[7] Pesso, T., Piva, S. (2009). Laminar natural convection in a square cavity: Low Prandtl numbers and large density differences. *Int. J. Heat Mass Transf*, 52 (3-4), 1036-1043. (DOI: 10.1016/j.ijheatmasstransfer.2008.07.005).

[8] Lopez, J. M., Marques, F., Avila, M. (2013). The Boussinesq approximation in rapidly rotating flows. *J. Fluid Mech*, 737, 56-77. (DOI: 10.1017/jfm.2013.558).

[9] Mayeli, P., Sheard, G.J., (2018). A comparison between Boussinesq and non-Boussinesq approximations for numerical simulation of natural convection in an annulus cavity. in *21st Australasian Fluid Mechanics Conference* Eds: T.C.W. Lau & R.M. Kelso, Pub: Australasian Fluid Mechanics Society, ISBN: 978-0-646-59784-3)), Adelaide Convention Centre, Adelaide, Australia.

[10] Mayeli, P., Sheard, G.J., (2020). A centrifugal buoyancy formulation for Boussinesq-type natural convection flows applied to the annulus cavity problem. *Int. J. Numer. Methods in Fluids*. In press.

[11] Ashrafizadeh, A., Alinia, B., Mayeli, P. (2015). A new co-located pressure-based discretization method for the numerical solution of incompressible Navier-Stokes equations, *Numer. Heat Transf, Part B*. 67 (6), 563-589. (DOI: 10.1080/10407790.2014.992094).

[12] Mayeli, P., Nikfar, M. (2019). Temperature identification of a heat source in conjugate heat transfer problems via an inverse analysis, *Int. J. Numerical Methods for Heat & Fluid Flow*. 29 (10) 3994-4010. (DOI: 10.1108/HFF-05-2018-0193).

[13] Hesami, H., Mayeli, P. (2016). Development of the ball-spine algorithm for the shape optimization of ducts containing nanofluid. *Numer. Heat Transf. A* 70 (12), 1371-1389. (DOI: 10.1080/10407782.2016.1243976).

[14] Mayeli, P., Nili-Ahmadabadi, M., Pirzadeh, M.R. Rahmani, P. (2017). Determination of desired geometry by a novel extension of ball spine algorithm inverse method to conjugate heat transfer problems. *Comput. Fluids*. 154, 390-406. (DOI: 10.1016/j.compfluid.2016.05.022).

[15] Mayeli, P., Nikfar, M. (2018). Surface shape design in different convection heat transfer problems via a novel coupled algorithm, *J. Heat Transf*. 140 (2): 021702. (DOI: 10.1115/1.4037581).

[16] Mayeli, P., Hesami, H., Besharati-Foumani, H. Niajalili, M. (2018). Al_2O_3–Water nanofluid heat transfer and entropy generation in a ribbed channel with wavy wall in the presence of magnetic field, *Numer. Heat Transf. Part A.* 73 (9) 604-623. (DOI: 10.1080/10407782.2018.1461494).

[17] Mayeli, P., Nili-Ahmadabadi, M., Besharati-Foumani, H. (2016). Inverse shape design for heat conduction problems via the ball spine algorithm, *Numer. Heat Transf. Part B*. 69 (3) 249-269. (DOI: 10.1080/10407790.2015.1096690).

[18] Mayeli, P., Hesami, H., Moghadam, MHDF. (2017). Numerical investigation of the MHD forced convection and entropy generation in a straight duct with sinusoidal walls containing water–Al_2O_3 nanofluid, *Numer. Heat Transf. Part A.* 71 (12) 1235-1250. (DOI: 10.1080/10407782.2017.1346998).